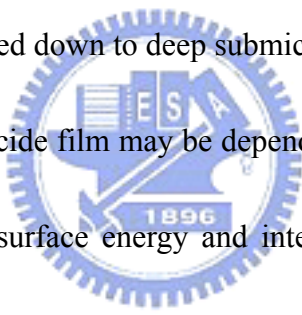


Chapter 2

Thermal stability of nickel silicide thin films on Si

2.1 Introduction

The application of metal-like silicides in integrated circuits is often limited by the thermal stability of the silicide film. The physical process of silicide degradation at high temperature includes the agglomeration of silicide film into discrete islands [1-3]. High temperature thermal stability of thin silicide film becomes an important issue as device dimension scaled down to deep submicron.



The degradation of silicide film may be dependent on the film thickness, grain size, grain boundary energy, surface energy and interface energy. There have been reported that small grain size, large surface and interface energy, and small grain boundary energy in the system of silicide/silicon may result in better resistance to silicide film agglomeration [4-6]. Thicker silicide film also has a better resistance to film agglomeration. In this chapter, we investigate the thermal stability of NiSi film employed in the ITS scheme which is used for silicide-contacted shallow junction formation.

2.2 Experimental procedures

The NiSi films studied in this work were formed on n-type and p-type (100)-oriented silicon wafers with 2.7~4 and 0.4~0.6 Ω -cm nominal resistivity, respectively. For the NiSi films formed on n-type silicon, a 150-Å-thick nickel (Ni) film was first sputter deposited on the n-type silicon substrate in a dc sputtering system with a base pressure of less than 2.5×10^{-8} torr, using a Ni target in Ar ambient at a pressure of 2×10^{-3} torr with a deposition rate of about 10 Å/sec. After the Ni film deposition, the samples were rapid thermal annealed (RTA) at 500°C for 30 sec in N₂ ambient to form nickel monosilicide (NiSi). The unreacted Ni film was selectively etched using a solution of H₂SO₄:H₂O₂=3:1 at 75~85°C. The formed NiSi film was about 310 Å in thickness as determined by cross-sectional transmission electron microscopy (TEM). Then, the samples of NiSi(310 Å)/Si were implanted with BF₂⁺ ions at an energy of 20-35 keV to a dose of 2×10^{15} or 5×10^{15} cm⁻². The ion implanted samples were then thermally annealed in a furnace (FA) at temperatures ranging from 550 to 800°C in N₂ ambient for 30 min or rapid thermal annealed (RTA) for a 30 sec duration at temperatures ranging from 600 to 800°C, also in N₂ ambient.

For the NiSi films formed on p-type silicon, a 300-Å-thick nickel (Ni) film was first sputter deposited on the p-type silicon substrate using the same sputter deposition conditions as those shown in the preceding paragraph. Then, this was followed by the same RTA process and selective etching of unreacted Ni film as those

shown in the preceding paragraph. The NiSi film formed was about 615 Å in thickness as determined by cross-sectional TEM. The samples of NiSi(615 Å)/Si were then received P⁺ implant or P⁺/F⁺ dual implant at various conditions as follows: P⁺ implant at an energy of 35 (sample P1) or 50keV (sample P2) to a dose of 5×10¹⁵ cm⁻², P⁺/F⁺ dual implant performed first with 35 keV/5×10¹⁵ cm⁻² P⁺ implantation followed by F⁺ implantation at 30 keV to a dose of 5×10¹⁵ cm⁻² (sample P1F5) or with 50keV/5×10¹⁵ cm⁻² P⁺ implantation followed by F⁺ implantation at 30keV to a dose of 2×10¹⁵ (sample P2F2), 4×10¹⁵ (sample P2F4) or 5×10¹⁵ cm⁻² (sample P2F5). The sample identification and the implantation conditions are summarized in Table 2.1. It has been reported that the presence of fluorine in silicide can promote the thermal stability of the silicide film [7]; thus the F⁺ implant is designed to improve the high temperature thermal stability of the P⁺ implanted NiSi film. The NiSi(615 Å)/Si samples formed by P⁺ implantation or P⁺/F⁺ dual implantation into/through the NiSi silicide were thermally annealed at temperatures ranging from 600 to 750°C for 90 min in N₂ ambient.

Simulation of ion implantation was performed using the TRIM program to estimate the as-implanted impurity profile in the NiSi layer and the Si substrate. The thicknesses of the as-deposited Ni films and the NiSi films formed were determined by cross-sectional TEM. Sheet resistance of the NiSi/Si samples was measured by a

four-point probe. The silicide surface and the Si surface after removal of the silicide layer were observed by scanning electron microscopy (SEM). Secondary ion mass spectrometry (SIMS) was used to determine the elemental concentration profile.

2.3 Results and discussion

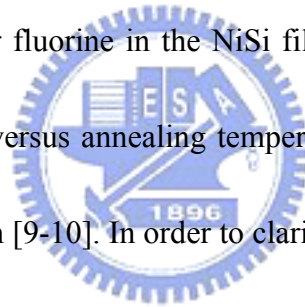
2.3.1 NiSi/Si sample implanted with BF_2^+ ions followed by FA

2.3.1.1 Sheet resistance measurement

Figure 2-1 and Fig. 2-2 shows the sheet resistance (R_s) as a function of annealing temperature for the NiSi(310 Å)/Si samples implanted with BF_2^+ at various energies to a dose of 2×10^{15} and $5 \times 10^{15} \text{ cm}^{-2}$, respectively; R_s data for the control sample without any ion implantation are also included for comparison. The R_s of the control sample started to show remarkable increase after annealing at temperatures above 600°C . This increase of R_s was apparently due to the formation of islands at high temperatures, resulting in discontinuous structure of the NiSi film, as confirmed by the SEM micrographs to be shown later in section 2.3.1.2. On the other hand, the R_s of the BF_2^+ implanted samples decreased slightly with increasing temperature up to 700°C . For the sample implanted with a lower dose of $2 \times 10^{15} \text{ cm}^{-2}$, annealing at 750°C resulted in NiSi film agglomeration and thus the increase of R_s , while the sample implanted with a higher dose of $5 \times 10^{15} \text{ cm}^{-2}$ was able to remain stable at

temperatures up to 750°C. The corresponding electrical resistivity of the NiSi film is about 18 $\mu\Omega\text{-cm}$, which is in agreement with the value reported in the literature [8].

For the NiSi(310 Å)/Si samples implanted with BF_2^+ at various energies to a higher dose of $5 \times 10^{15} \text{ cm}^{-2}$, the increase in Rs after annealing at 800°C is attributed to NiSi_2 phase formation. On the other hand, for the NiSi(310 Å)/Si samples implanted with BF_2^+ at various energies to a dose of $2 \times 10^{15} \text{ cm}^{-2}$, a specific decrease in Rs after annealing at 800°C was observed in this work. This will be discussed in the following section 2.3.1.2 with regard to the NiSi_2 formation and the thin film stress. The incorporation of boron and/or fluorine in the NiSi film is apparently responsible for the different behavior of Rs versus annealing temperature between the samples with and without BF_2^+ implantation [9-10]. In order to clarify this point, further experiment was conducted as in the following. The NiSi(310 Å)/Si samples were implanted with BF_2^+ , B^+ and F^+ ions separately at equivalent energies and doses as follows: 50 keV/ $2 \times 10^{15} \text{ cm}^{-2}$ for BF_2^+ , 12 keV/ $2 \times 10^{15} \text{ cm}^{-2}$ for B^+ , and 20 keV/ $4 \times 10^{15} \text{ cm}^{-2}$ for F^+ implantation. The sheet resistance versus annealing temperature for these samples is illustrated in Fig. 2-3. It can be seen that the Rs values as well as the behavior of Rs versus annealing temperature for the BF_2^+ -implanted and the F^+ -implanted samples are fairly similar, while the control sample and the B^+ -implanted sample exhibited a drastic increase in Rs at temperatures above 600 and 700°C, respectively. These



results strongly imply that the amelioration in the sheet resistance of thin NiSi film is apparently due to the incorporation of fluorine atom into the film.

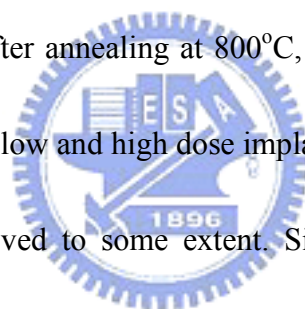
Figure 2-4 shows the SIMS depth profiles of fluorine in the sample of NiSi(310 Å)/Si implanted with BF_2^+ at 35 keV to a dose of 2×10^{15} as well as 5×10^{15} cm^{-2} followed by thermal annealing at 750°C. It was reported that higher fluorine concentration in the silicide grain and/or at the silicide/silicon interface will improve the silicide thermal stability [7]. In this study, our experimental results obtained from the sheet resistance measurement clearly indicate the thermal stability improvement of the NiSi film by appropriate incorporation of fluorine atoms via ion implantation into the NiSi/Si sample.



2.3.1.2 Surface morphology of BF_2^+ implanted NiSi/Si samples

Figure 2-5 shows the surface morphology of the NiSi(310 Å)/Si control sample annealed at various temperatures. Film agglomeration occurred at temperatures as low as 600°C. The NiSi film was turned into isolated islands after annealing at and above 700°C, resulting in a remarkable increase in the measured sheet resistance (Fig. 2-1 and Fig. 2-2). Figure 2-6 shows the surface morphology of the BF_2^+ (35 keV) implanted NiSi(310 Å)/Si samples annealed at temperatures of 700 to 800°C. For the lower dose (2×10^{15} cm^{-2}) implanted sample, the NiSi film remained

smooth after annealing at 700°C, but film agglomeration was observed after annealing at 750°C, which might cause NiSi/Si interface roughness. For the higher dose ($5 \times 10^{15} \text{ cm}^{-2}$) implanted sample, the NiSi film remained stable at temperatures up to 750°C. Similar results were observed for the samples implanted with BF_2^+ at lower energies of 25 and 30 keV. Apparently, incorporation of fluorine in NiSi film in a larger amount promoted the retardation of the NiSi film agglomeration. We presume that the segregation of the implanted fluorine species at the NiSi grain boundaries resulted in the change of grain boundary energy and interfacial energy, leading to the retardation of the film agglomeration. After annealing at 800°C, localized sinking was observed on the silicide surface of both low and high dose implanted samples, and the degree of film agglomeration was relieved to some extent. Since NiSi_2 phase was found to appear after annealing at 800°C, and it consumes more Si ($\text{Ni} : \text{Si} : \text{NiSi}_2 = 1 \text{ \AA} : 3.65 \text{ \AA} : 3.63 \text{ \AA}$) than the formation of NiSi phase ($\text{Ni} : \text{Si} : \text{NiSi} = 1 \text{ \AA} : 1.83 \text{ \AA} : 2.34 \text{ \AA}$) [8], the localized newly formed NiSi_2 surface would sink. Moreover, the lattice constant of NiSi_2 (5.406 Å) is closer to that of Si (5.43 Å) than that of NiSi (4.445 Å), which corresponds to a less film stress and better resistance to the film agglomeration. Furthermore, we presume that the phase transformation of NiSi to NiSi_2 occurred before the NiSi-based agglomeration during the 30 min annealing at 800°C. Thus, the drop in R_s for the lower dose ($2 \times 10^{15} \text{ cm}^{-2}$) implanted sample as the annealing



temperature was raised from 750 to 800°C (Fig. 2-2) could be attributed to the smoother Ni-silicide film. We may conclude that the formation of NiSi₂ relaxed the agglomeration of silicide film, making it possible to maintain the continuity of the silicide film. The BF₂⁺ implantation improves the thermal stability of NiSi film as confirmed by the films sheet resistance behavior and the smoother surface morphology.

Figure 2-7 shows the surface morphology of the Si substrate after removal of the NiSi film from the thermally annealed NiSi/Si samples. It can be seen that severe silicide film agglomeration had occurred for the control sample, causing a very rough silicide/Si interface. For the lower dose ($2 \times 10^{15} \text{ cm}^{-2}$) implanted sample, the silicon surface remained intact after 700°C annealing, but became pitted after annealing at 750°C. For the higher dose ($5 \times 10^{15} \text{ cm}^{-2}$) implanted sample, the silicide/Si interface remained smooth even up to a temperature of 750°C. Evidently, the roughness of the silicide/Si interface was alleviated by the incorporation of fluorine atoms with a BF₂⁺ implantation dose of $2 \times 10^{15} \text{ cm}^{-2}$, and the interface roughness was almost avoided when the BF₂⁺ implantation dose was raised to $5 \times 10^{15} \text{ cm}^{-2}$.

2.3.2 NiSi/Si sample implanted with BF₂⁺ ions followed by RTA

2.3.2.1 Sheet resistance measurement

Figure 2-8 shows the sheet resistance (R_s) as a function of RTA temperature for the BF_2^+ -implanted $\text{NiSi}(310 \text{ \AA})/\text{Si}$ samples; R_s data for the control sample without any ion implantation are also included for comparison. The R_s of the control sample started to show remarkable increase after annealing at temperatures above 750°C . This increase of R_s is apparently due to the formation of islands at high temperatures, resulting in discontinuous structure of the NiSi film, as confirmed by the SEM micrographs to be shown in the following section. The remarkable increase in R_s due to possible contribution from the high resistive NiSi_2 phase is excluded because the X-ray diffraction (XRD) analysis did not reveal the formation of NiSi_2 after RTA at temperatures up to 800°C . On the other hand, the R_s of the BF_2^+ -implanted samples decreased slightly with increasing temperature, presumably due to recovery of the implantation induced defects; nonetheless, it remained stable up to 800°C , and the corresponding electrical resistivity of the fluorine contained NiSi film is about $21\sim 22 \mu\Omega\text{-cm}$, which is slightly higher than the value reported in the literature for the bulk NiSi ($14\sim 20 \mu\Omega\text{-cm}$) [8]. The different behavior of R_s value versus annealing temperature for the sample with and without BF_2^+ -implantation is attributed to the incorporation of fluorine in the NiSi film, leading to the retardation of film agglomeration [7, 10].

2.3.2.2 Surface morphology of BF_2^+ implanted NiSi/Si samples

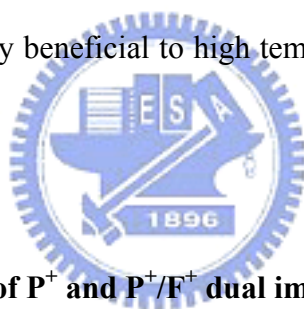
Figure 2-9 illustrates the SEM micrographs showing surface morphology of the NiSi/Si samples annealed with RTA at various temperatures. For the control sample, the NiSi film became agglomerate at a temperature as low as 650°C, and the film was turned into isolated islands after annealing at 800°C, resulting in a remarkable increase in the measured sheet resistance (Fig. 2-8). In contrast, the NiSi film of the BF_2^+ ($35 \text{ keV}/5 \times 10^{15} \text{ cm}^{-2}$) implanted sample remained intact after annealing at temperatures up to 800°C (Fig. 2-9(d)). Similar results were observed for the samples implanted with BF_2^+ at lower energies of 20 to 30 keV.

2.3.3 NiSi/Si sample implanted with P^+ ions followed by FA

2.3.3.1 Sheet resistance measurement

Figure 2-10 shows the sheet resistance (R_s) as a function of furnace annealing (FA) temperature for the P^+ -implanted and P^+/F^+ -dual-implanted NiSi/Si samples; R_s data for the control sample without any ion implantation are also included for comparison. The R_s of the control, P1, and P2 samples started to increase at temperatures above 650°C. This increase of R_s is presumably due to the NiSi film's agglomeration and formation of islands at high temperatures, as confirmed by the SEM micrographs to be shown later in section 2.3.3.2. Moreover, the formation of highly resistive NiSi_2 phase at 750°C, as shown in Fig. 2-11, led to the drastic increase

of Rs. For the fluorine containing samples (P1F5, P2F2, P2F4, and P2F5), the Rs remained stable up to 750°C except the sample P2F2, which was implanted with the least amount of F⁺ ions and exhibited a small increase in Rs due to agglomeration of the NiSi film. The fact that the P1F5, P2F4 and P2F5 samples are thermally stable up to 750°C is apparently due to incorporation of sufficient amount of fluorine atoms in the NiSi film, resulting in the retardation of film agglomeration and NiSi₂ formation. Figure 2-12 shows the SIMS depth profile of fluorine atoms in the sample of P2F5 annealed at 750°C. The high concentration of fluorine in the NiSi film and at the NiSi/Si interface is presumably beneficial to high temperature thermal stability of the NiSi/Si system.



2.3.3.2 Surface morphology of P⁺ and P⁺/F⁺ dual implanted NiSi/Si samples

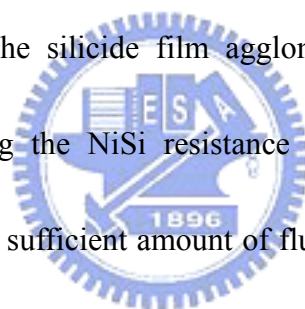
Figure 2-13 shows the surface morphology of NiSi(615 Å)/Si control sample annealed at various temperatures, which is similar to, but not exactly the same as the surface morphology of the thermally annealed NiSi(310 Å)/Si control sample shown in Fig. 2-5 because of the different thickness of the NiSi film and the longer duration of annealing (90 min). Film agglomeration occurred at a temperature as low as 600°C, and the NiSi film was turned to isolated islands after annealing at and above 700°C, resulting in a drastic increase of the measured sheet resistance (Fig. 2-10). Figure 2-14 shows the surface morphology of P2, P2F2, P2F4 and P2F5 samples annealed at

750°C. The NiSi film of the phosphorus implanted P2 sample started to agglomerate at 700°C and was turned to isolated islands after annealing at 750°C. The incorporation of fluorine atoms retarded or even prohibited the film agglomeration, as evidenced by the samples P2F2, P2F4 and P2F5, in particular the sample P2F5, whose surface remained intact after annealing at 750°C. Similar results were observed for P1 and P1F5 samples. Figure 2-15 shows the surface morphology of the Si substrate after removal of the silicide layer for P2, P2F2, P2F4, P2F5, and P1F5 samples annealed at 750°C. Large pits appeared on the Si substrate surface for P2 sample, apparently due to severe agglomeration of the NiSi film. For the F⁺ implanted samples, the silicide/Si interface became smoother and the roughness of the Si surface was alleviated; the Si substrate surface contained fewer and smaller pits for the samples implanted with higher dose of F⁺ ions (samples P2F4 and P2F5). The Si substrate surface of P1F5 sample turned out to be the smoothest one among the samples studied in this work. Table 2.2 summarizes the NiSi phase detected in the sample of NiSi/Si with/without BF₂⁺, P⁺ and P⁺/F⁺ implantation followed by annealing treatment at various temperatures.

2.4 Conclusions

The thermal stability of thin NiSi film with respect to ion implantation is

studied in this chapter. The BF_2^+ implantation improves the high temperature thermal stability of the thin NiSi silicide film due to the incorporation of fluorine atoms. It is presumed that fluorine atoms segregated to the NiSi grain boundaries, forming Si-F and Ni-F strong bonding and resulting in the suppression of silicide agglomeration by decreasing the interfacial energy, i.e. stress between the silicide layer and silicon substrate; thus, the integrity of the silicide layer can be preserved at high temperatures. For the P^+ -implanted samples, the R_s value degraded after thermal annealing at 700°C . The incorporation of fluorine atoms by using P^+/F^+ dual implantation was able to retard and/or even prevent the silicide film agglomeration. We conclude that an effective means of upgrading the NiSi resistance to film agglomeration at high temperatures is to introduce a sufficient amount of fluorine atoms in the NiSi silicide film and at the NiSi/Si interface.



References

1. H. Jeon and R. J. Nemanich, *Thin Solid Films* **184**, 357 (1984).
2. H. Jeon, C. A. Sukow, J. W. Honeycutt, G. A. Rozgonyi, and R. J. Nemanich, *J. Appl. Phys.* **71**, 4269 (1992).
3. K. Shenai, *J. Mater. Res.* **6**, 1502 (1991).
4. P. Revesz, L. R. Zheng, L. S. Hung, and J. W. Mayer, *Appl. Phys. Lett.* **48**, 1591 (1986).
5. T. P. Nolan, R. Sinclair, and R. Beyers, *J. Appl. Phys.* **71**, 720, (1992).
6. Z. G. Xiao, G. A. Rozgonyi, C. A. Canovai, and C. M. Osburn, *Mater. Res. Soc. Symp.* **202**, 101 (1991).
7. A. S. W. Wong, D. Z. Chi, M. Loomans, D. Ma, M. Y. Lai, W. C. Tjiu, S. J. Chua, C. W. Lim, and J. E. Greene, *Appl. Phys. Lett.* **81**, 5138 (2002).
8. S. P. Murarka, *Silicides for VLSI Applications*, Academic, New York (1983), p. 130.
9. S. S. Lau and N. W. Cheung, *Thin Solid Films* **71**, 117 (1980).
10. B. Y. Tsui, J. Y. Tsai, T. S. Wu, and M. C. Chen, *IEEE Trans. Electron Device* **40**, 54 (1993).

Table 2.1 Sample identification and implantation conditions for the NiSi(615Å)/Si samples.

Sample ID	Implantation Condition (energy/dose)
P1	P ⁺ 35keV/5×10 ¹⁵ cm ⁻²
P2	P ⁺ 50keV/5×10 ¹⁵ cm ⁻²
P1F5	P ⁺ 35keV/5×10 ¹⁵ cm ⁻² followed by F ⁺ 30keV/5×10 ¹⁵ cm ⁻²
P2F2	P ⁺ 50keV/5×10 ¹⁵ cm ⁻² followed by F ⁺ 30keV/2×10 ¹⁵ cm ⁻²
P2F4	P ⁺ 50keV/5×10 ¹⁵ cm ⁻² followed by F ⁺ 30keV/4×10 ¹⁵ cm ⁻²
P2F5	P ⁺ 50keV/5×10 ¹⁵ cm ⁻² followed by F ⁺ 30keV/5×10 ¹⁵ cm ⁻²



Table 2.2 Nickel silicide phase in the sample of NiSi/Si with/without BF_2^+ , P^+ and P^+/F^+ implantation followed by annealing treatment at various temperatures.

		550°C	600~700°C	750°C	800°C
Non-implanted	RTA (30s)		NiSi	NiSi	NiSi, NiSi ₂
	FA (30min)	NiSi	NiSi	NiSi	NiSi, NiSi ₂
BF_2^+ -implanted	RTA (30s)		NiSi	NiSi	NiSi, NiSi ₂
	FA (30min)	NiSi	NiSi	NiSi	NiSi, NiSi ₂
P^+ -implanted	FA (90min)		NiSi	NiSi, NiSi ₂	
P^+/F^+ dual implanted	FA (90min)		NiSi	NiSi	



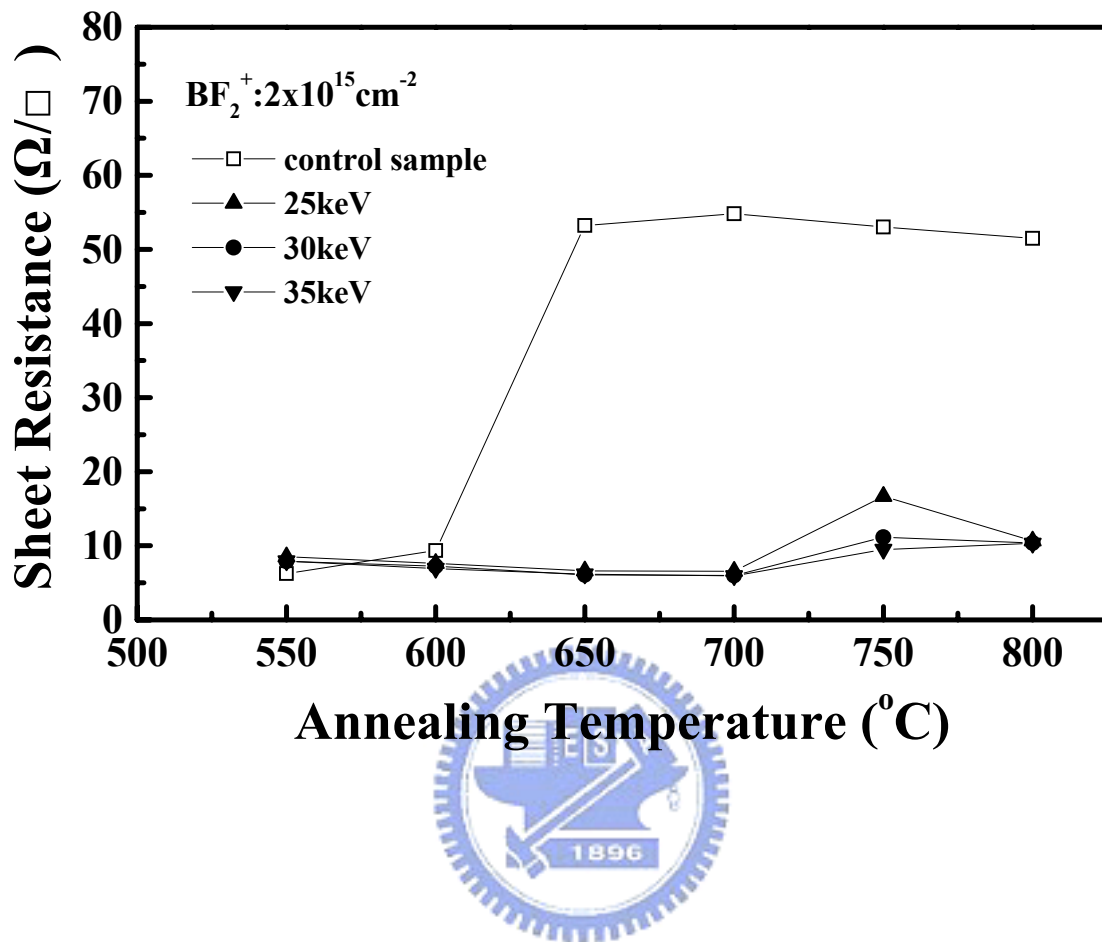


Fig. 2-1 Sheet resistance vs. annealing temperature for NiSi(310Å)/Si samples implanted with BF₂⁺ at various energies to a dose of 2×10¹⁵cm⁻². The sample without ion implantation is designated as control sample.

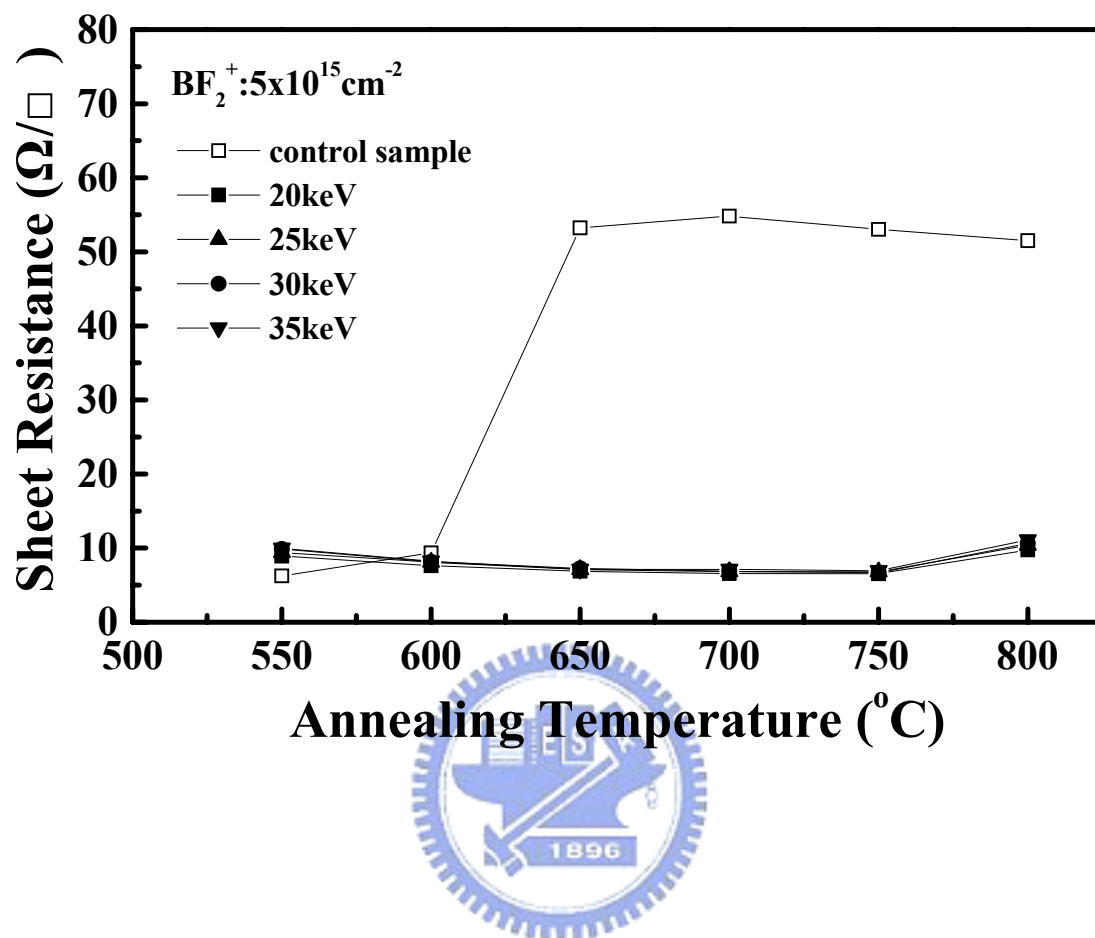


Fig. 2-2 Sheet resistance vs. annealing temperature for NiSi(310Å)/Si samples implanted with BF₂⁺ at various energies to a dose of 5×10¹⁵cm⁻². The sample without ion implantation is designated as control sample.

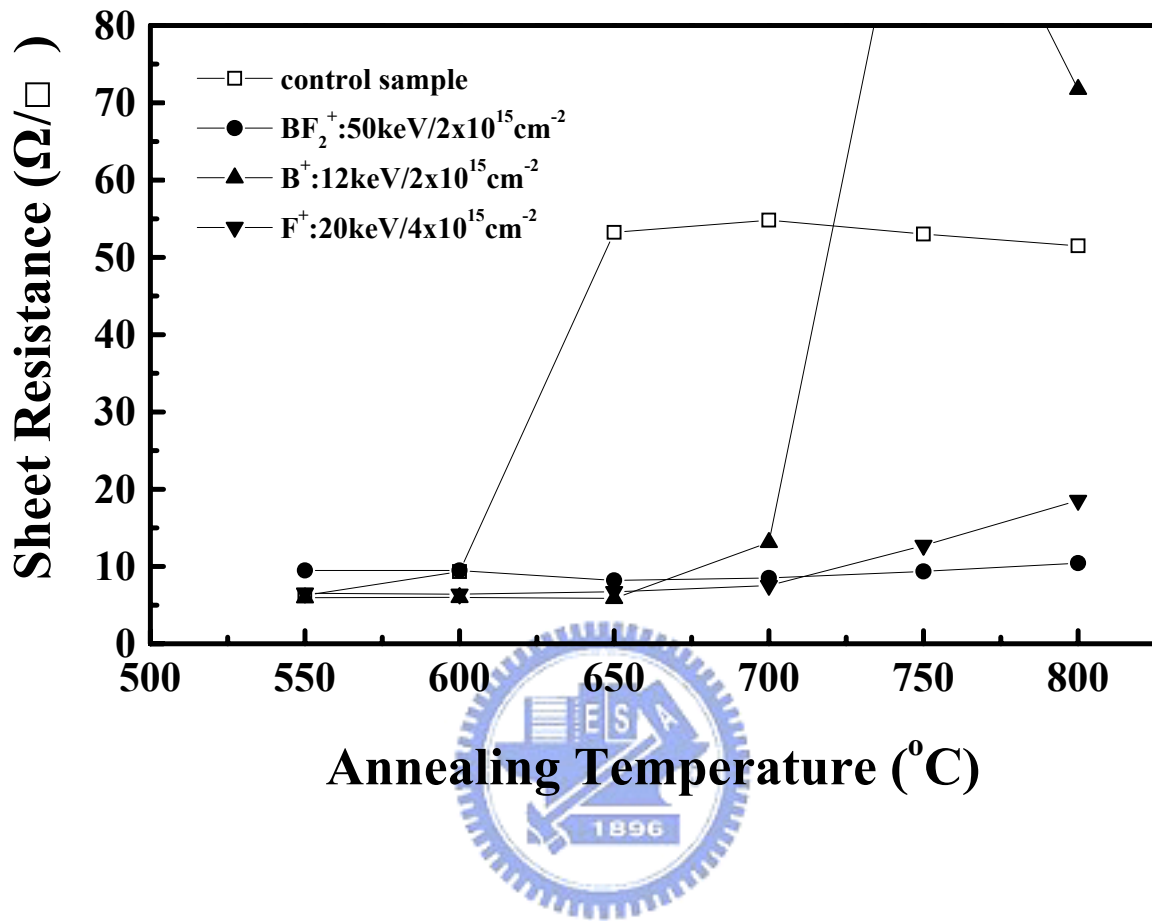


Fig. 2-3 Sheet resistance vs. annealing temperature for NiSi(310Å)/Si samples implanted with BF₂⁺, B⁺, and F⁺ ions. The control sample stands for the NiSi(310Å)/Si sample without any ion implantation.

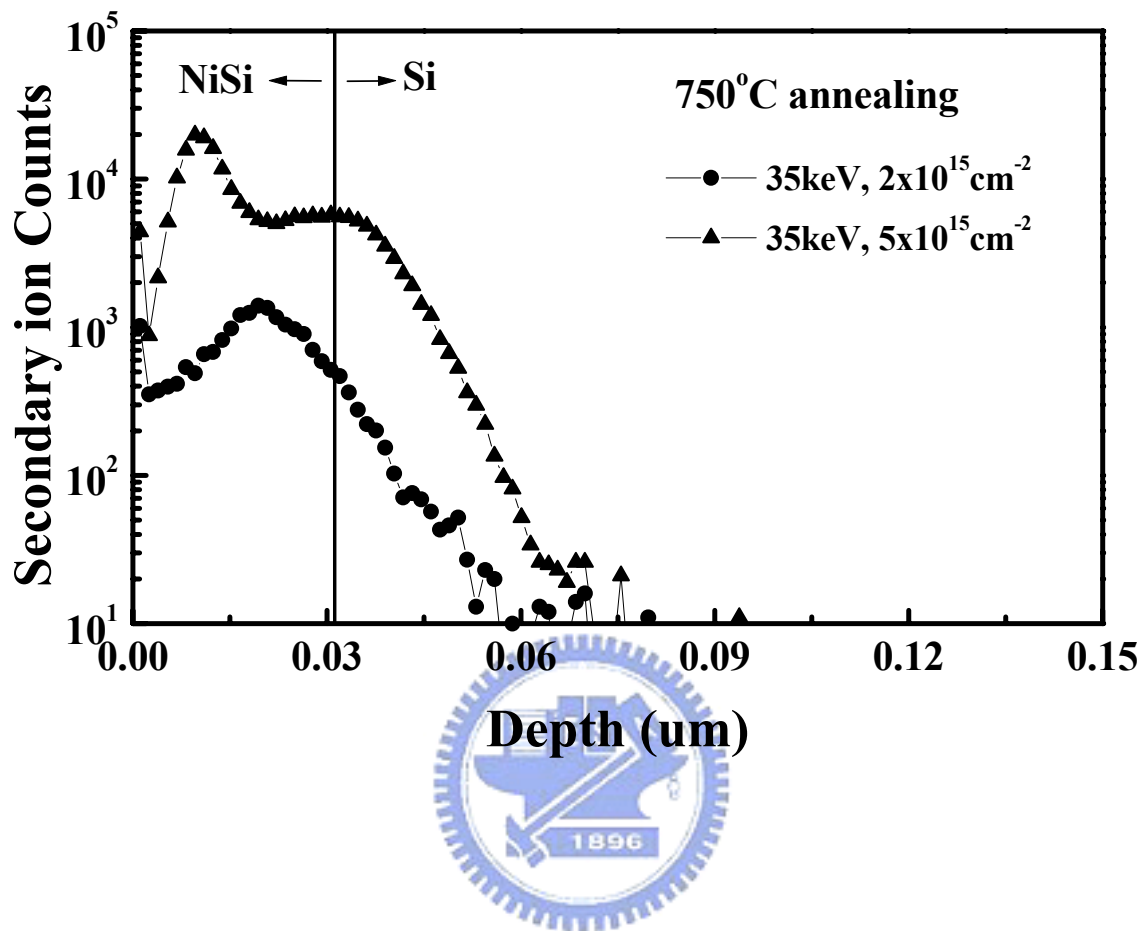


Fig. 2-4 SIMS depth profiles of fluorine in NiSi(310Å)/Si samples implanted with BF_2^+ at 35 keV to a dose of 2×10^{15} as well as $5 \times 10^{15} \text{ cm}^{-2}$ followed by 750°C thermal annealing.

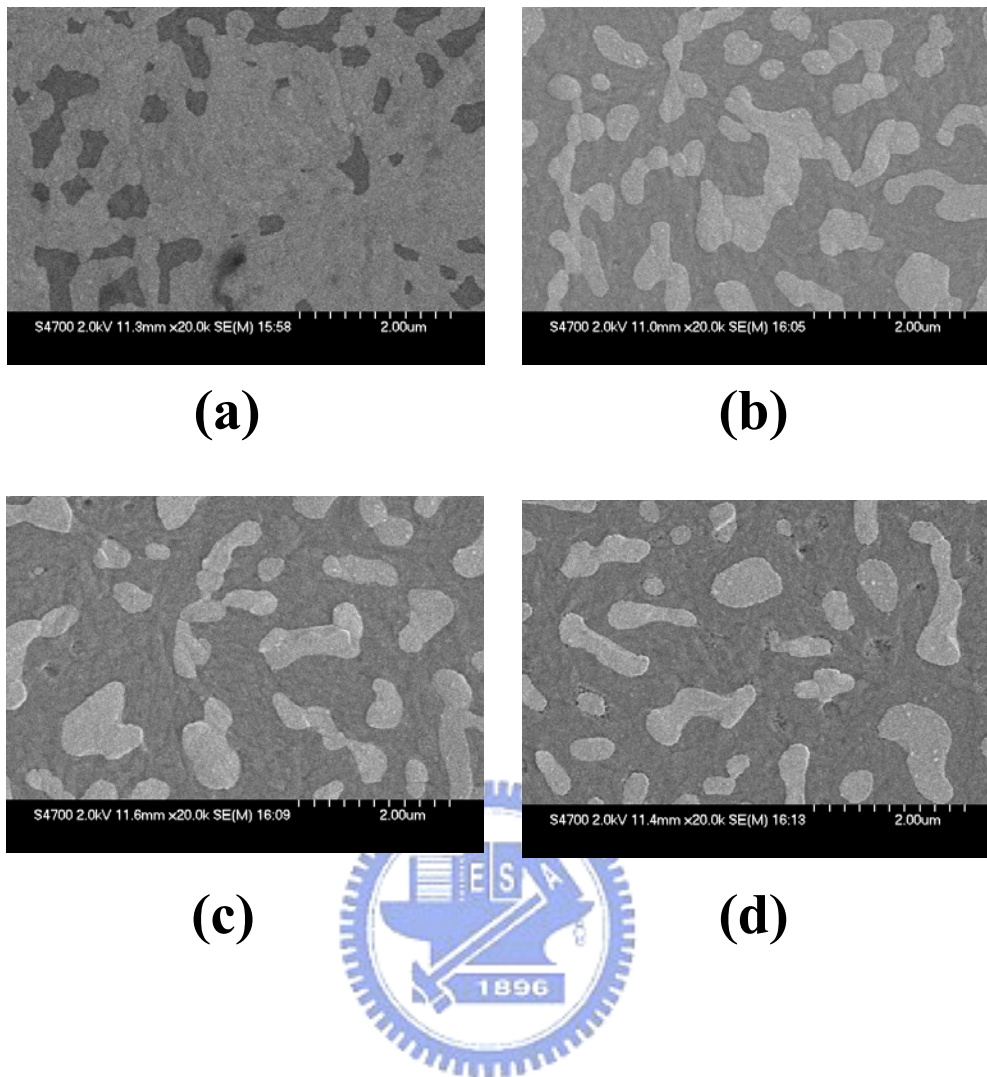


Fig. 2-5 Top view SEM micrograph showing the surface morphology of non-implanted NiSi(310Å)/Si control sample annealed at (a) 600, (b) 700 (c) 750, and (d) 800°C for 30 min.

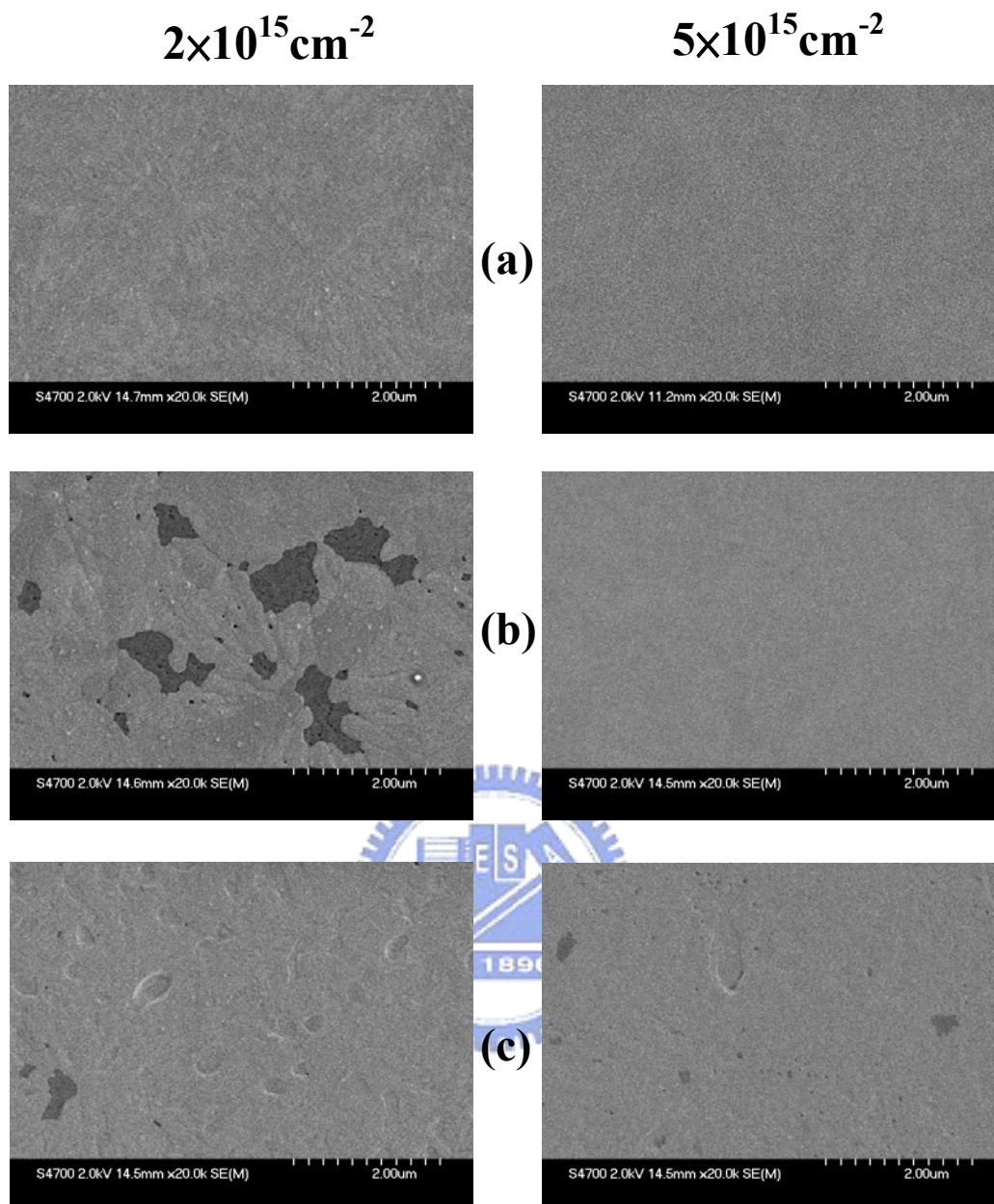


Fig. 2-6 SEM micrographs showing the surface morphology of BF_2^+ (35keV) implanted NiSi (310Å)/Si samples annealed at (a) 700, (b) 750, and (c) 800°C for 30 min. The low-dose ($2 \times 10^{15} \text{ cm}^{-2}$) and high-dose ($5 \times 10^{15} \text{ cm}^{-2}$) implanted samples are shown on the left and right columns, respectively.

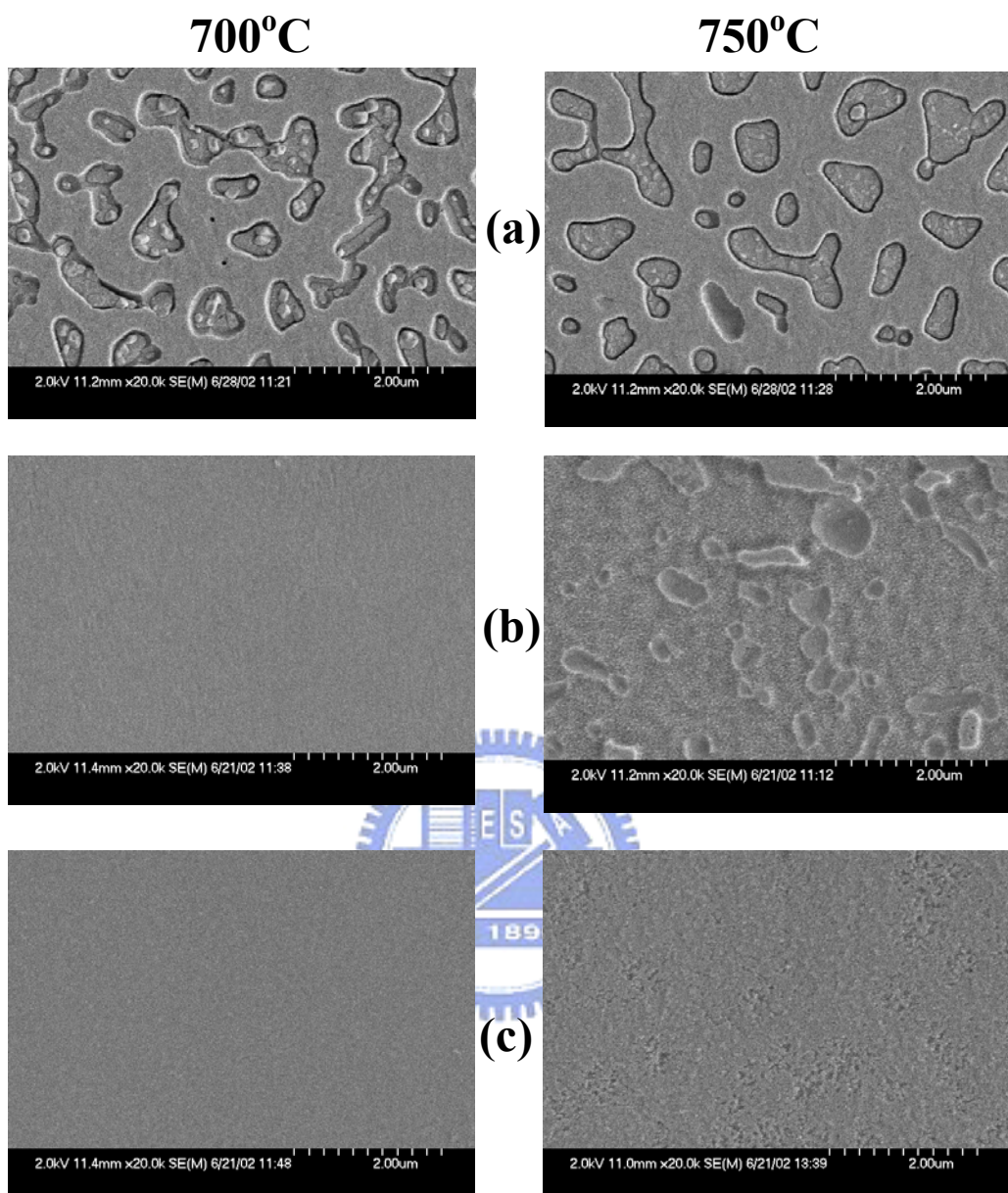


Fig. 2-7 SEM micrographs showing the surface morphology of Si substrate after removal of NiSi film from the 700 (left) and 750°C (right) annealed NiSi/Si samples: (a) control sample, (b) sample implanted with BF_2^+ at 35keV to a dose of $2 \times 10^{15} \text{cm}^{-2}$, and (c) sample implanted with BF_2^+ at 35keV to a dose of $5 \times 10^{15} \text{cm}^{-2}$.

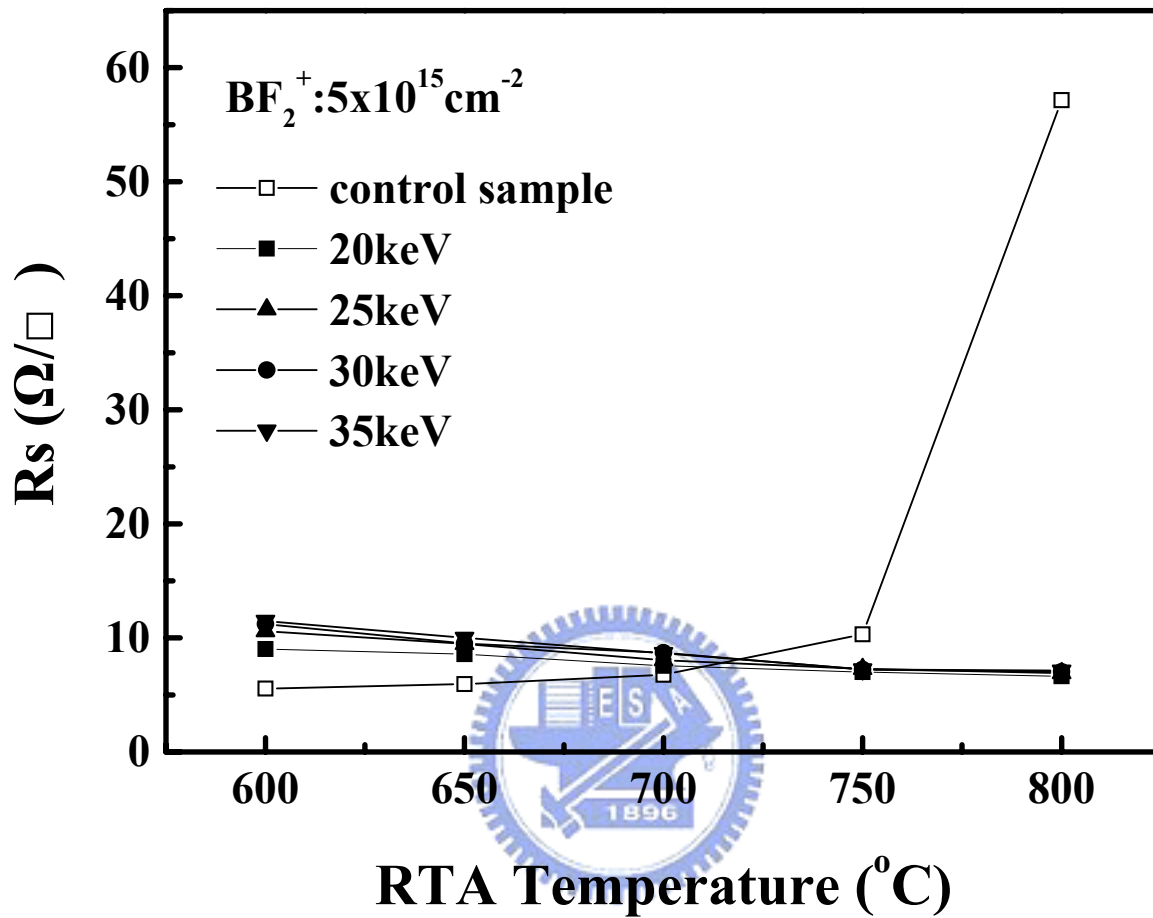


Fig. 2-8 Sheet resistance vs. RTA temperature for NiSi(310Å)/Si samples implanted with BF₂⁺ at various energies to a dose of 5×10¹⁵cm⁻². The sample without ion implantation is designated as control sample.

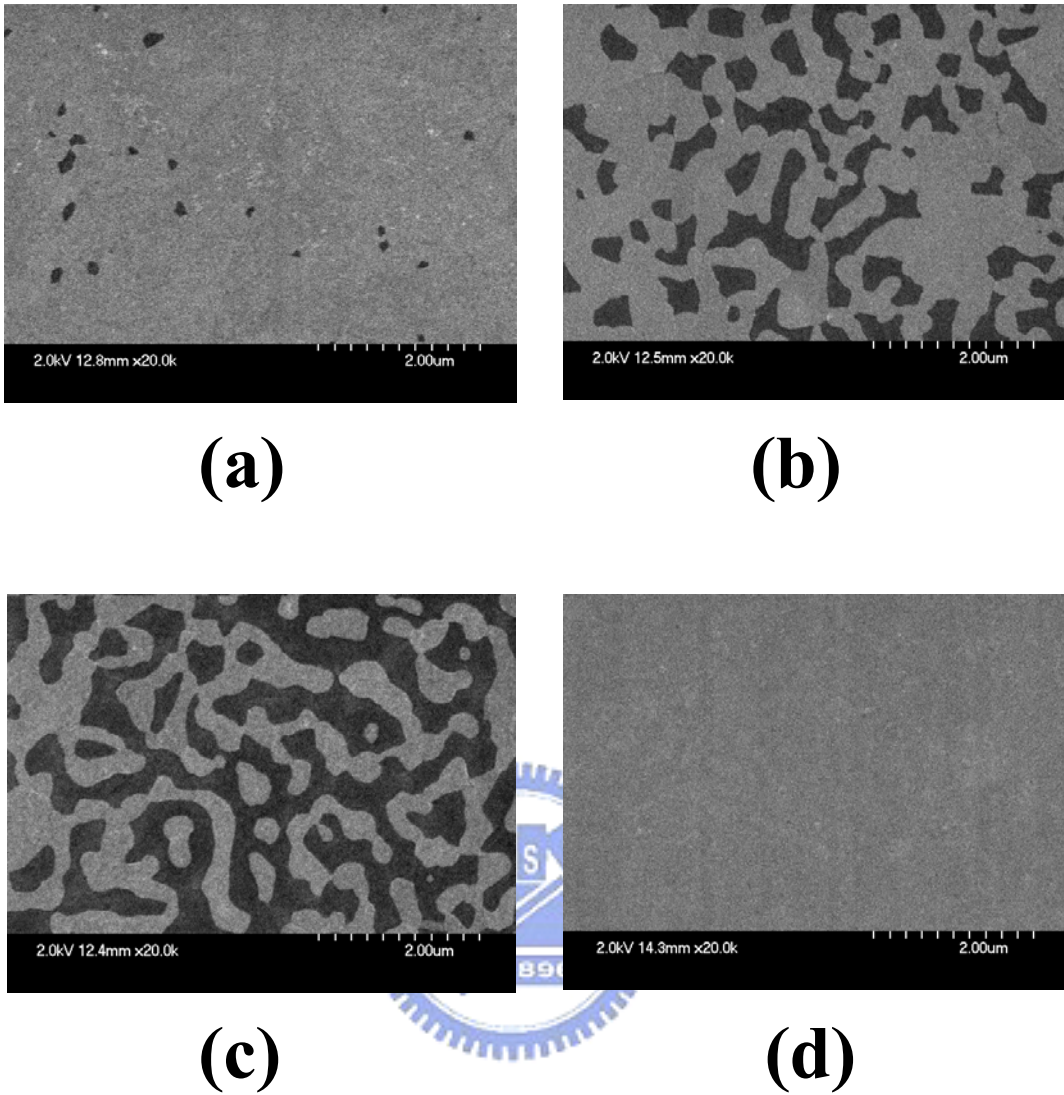


Fig. 2-9 Top view SEM micrographs showing surface morphology of NiSi(310Å)/Si samples annealed with RTA for 30 sec at various temperatures: (a) control sample at 650°C, (b) control sample at 750°C, (c) control sample at 800°C, and (d) BF₂⁺ (35keV) implanted sample at 800°C.

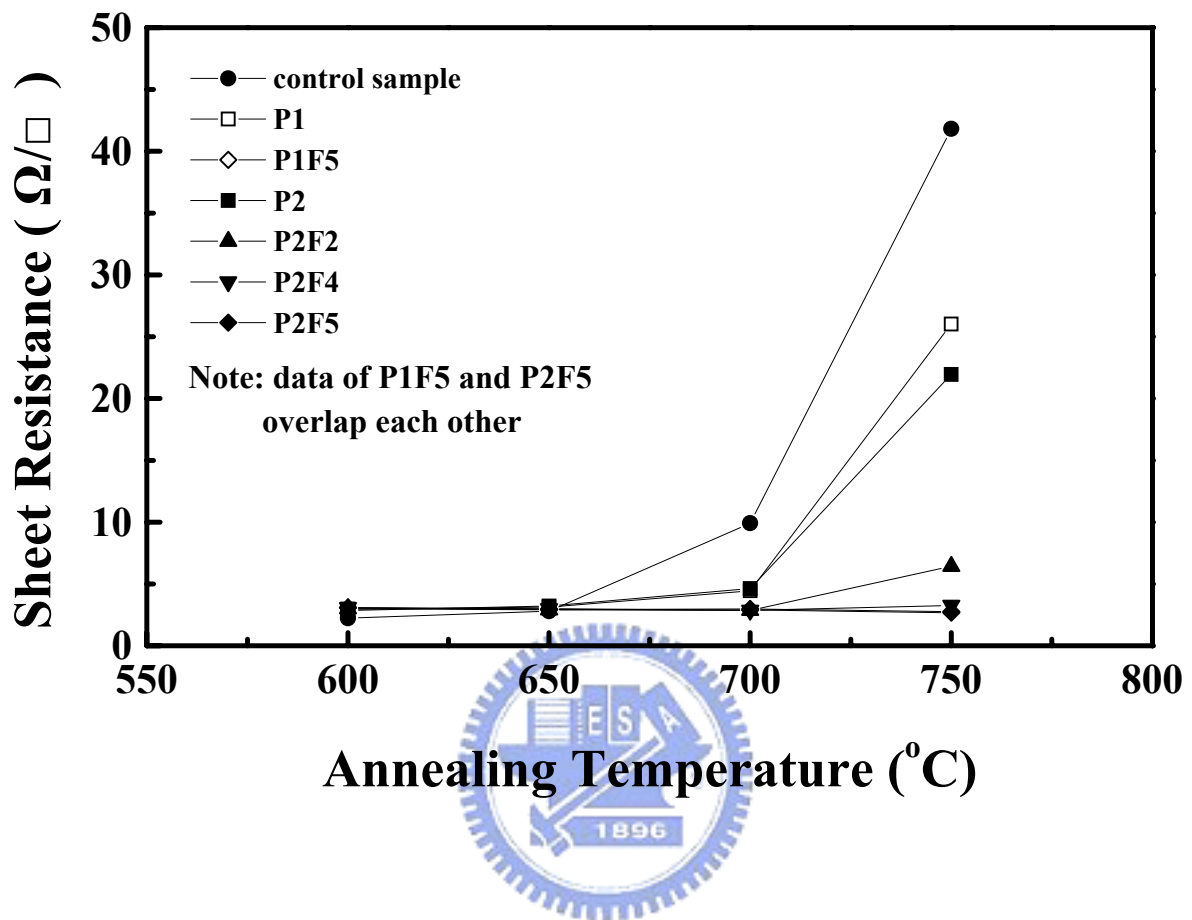


Fig. 2-10 Sheet resistance vs. annealing temperature for NiSi(615Å)/Si samples implanted with P⁺ (single implantation) and P⁺/F⁺ (dual implantation) at various implantation conditions. The sample without any ion implantation is designated as control sample.

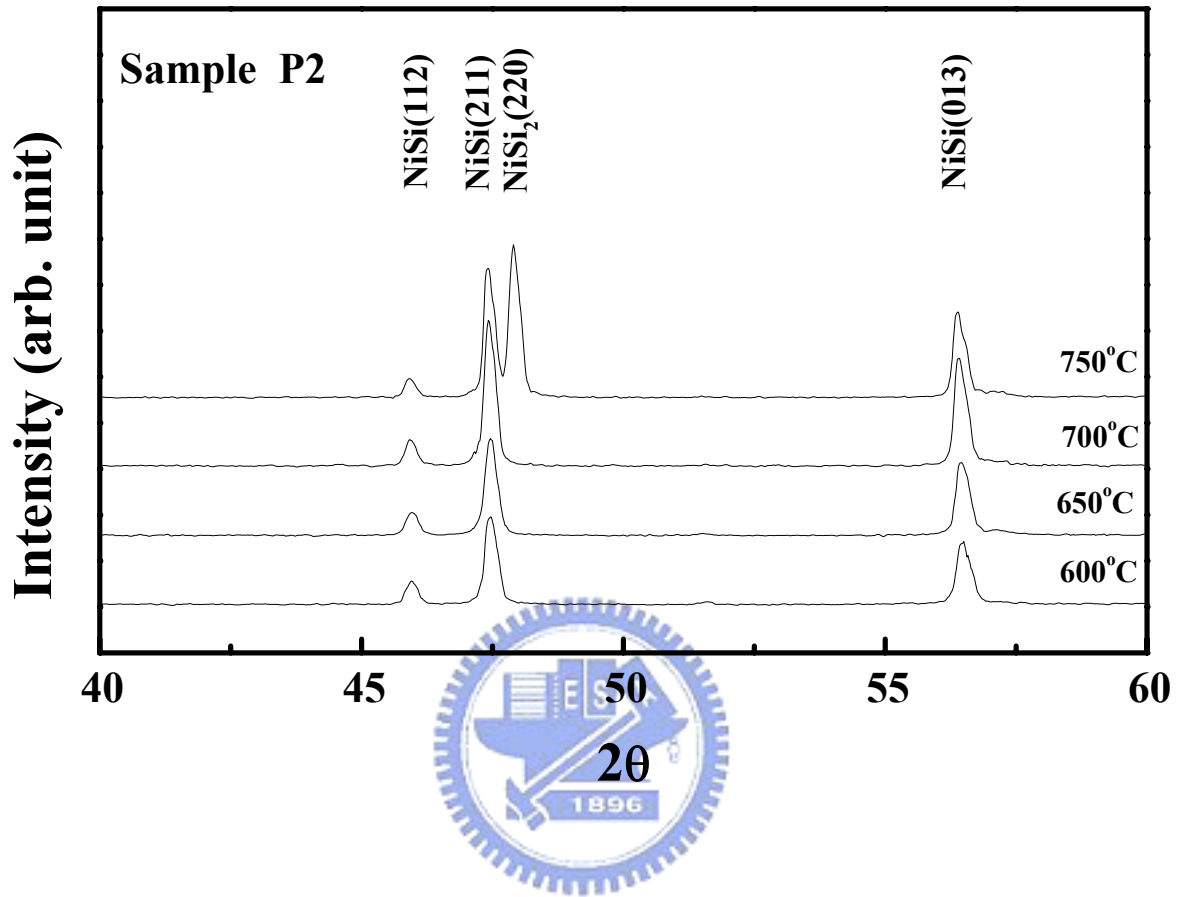


Fig. 2-11 XRD spectra for sample P2 (implanted with P⁺ ions at 50keV to a dose of $5 \times 10^{15} \text{ cm}^{-2}$) annealed at various temperatures. NiSi₂ phase appears after annealing at 750°C.

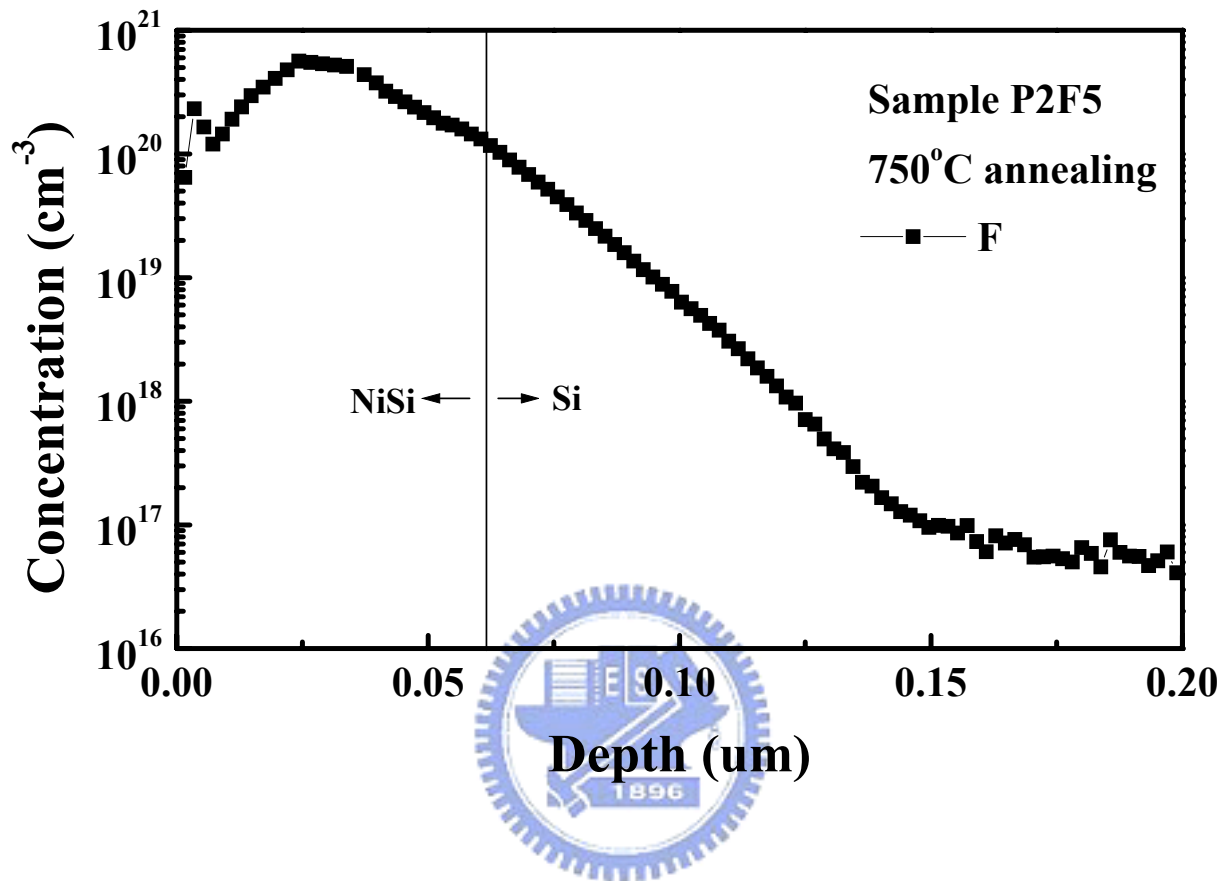
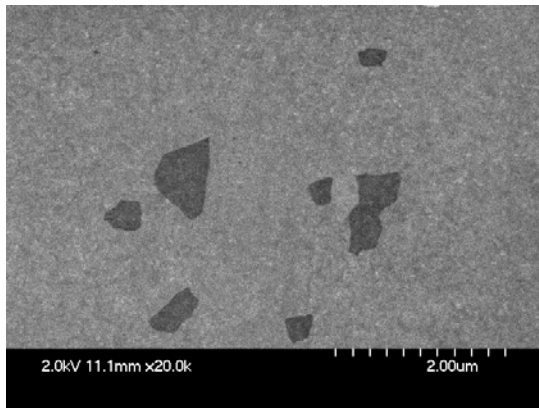
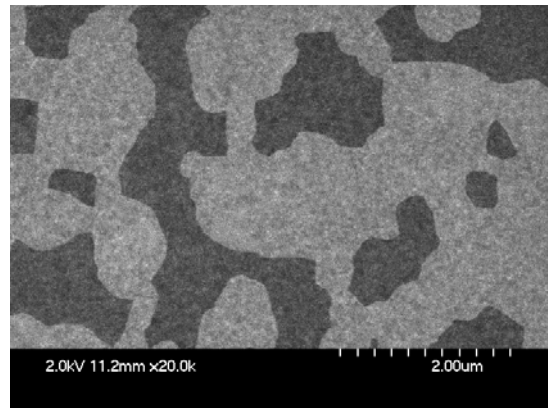


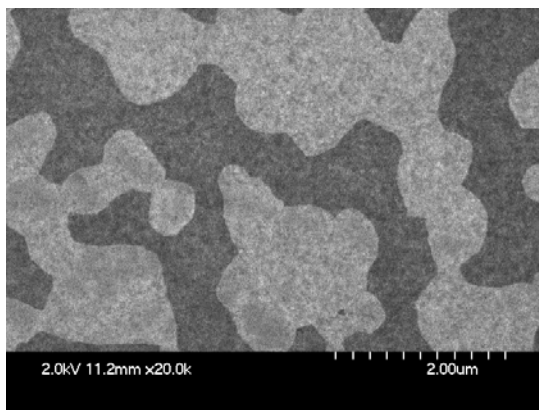
Fig. 2-12 SIMS depth profile of fluorine in sample P2F5 (dual implantation with P⁺/F⁺ ions at 50/30 keV to a dose of 5×10¹⁵/5×10¹⁵ cm⁻²) annealed at 750°C.



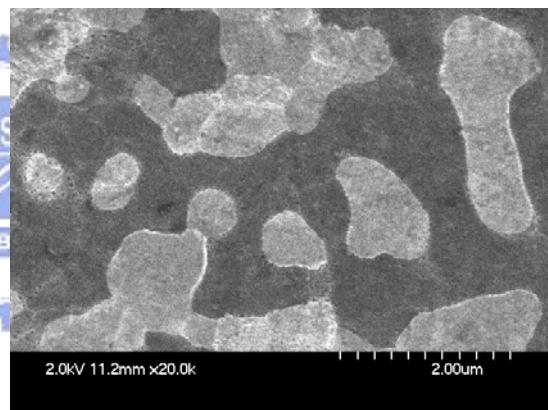
(a)



(b)

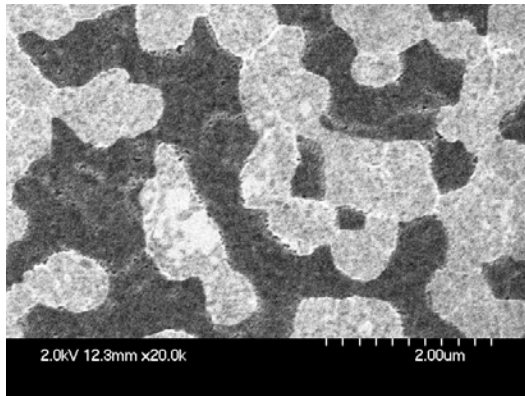


(c)

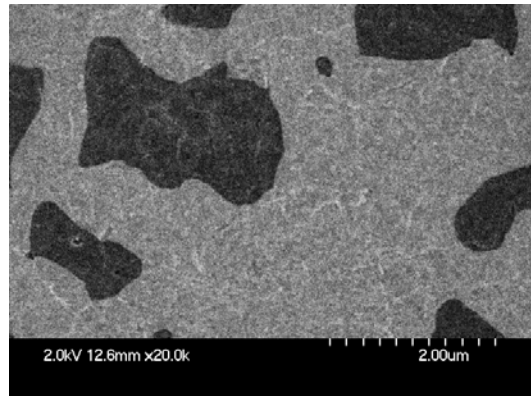


(d)

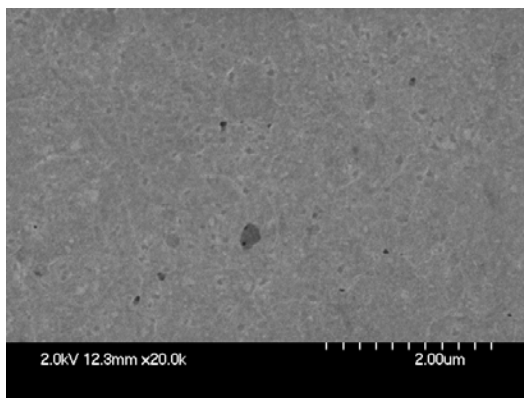
Fig. 2-13 SEM micrographs showing surface morphology of NiSi(615Å)/Si control sample annealed at (a) 600, (b) 650, (c) 700, and (d) 750°C for 90 min.



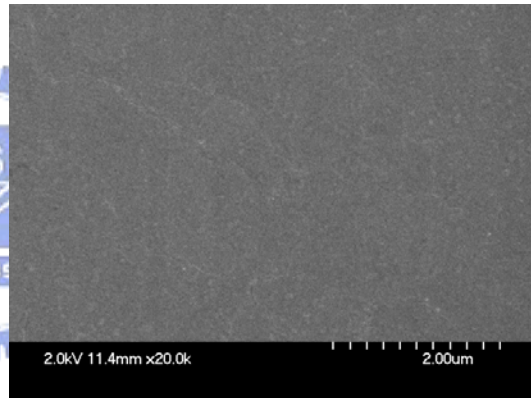
(a)



(b)

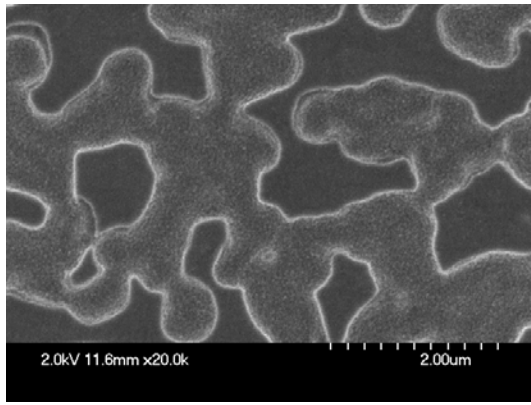


(c)

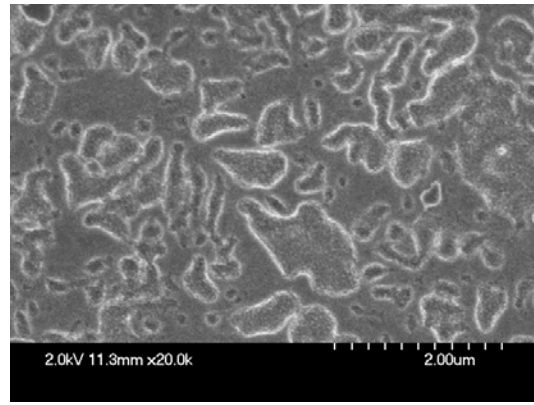


(d)

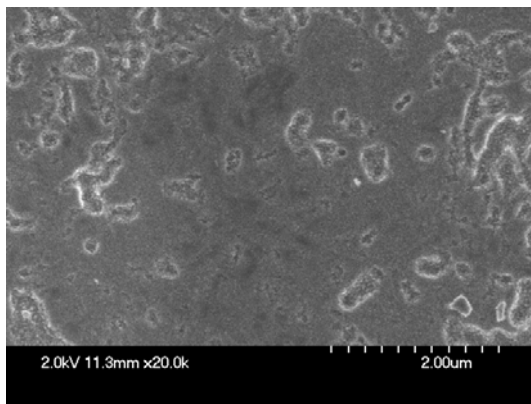
Fig. 2-14 SEM micrographs showing surface morphology of ion implanted NiSi/Si samples of (a) P2, (b) P2F2, (c) P2F4, and (d) P2F5 annealed at 750°C for 90 min.



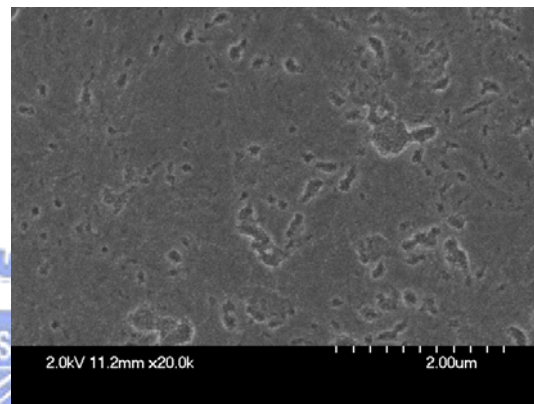
(a)



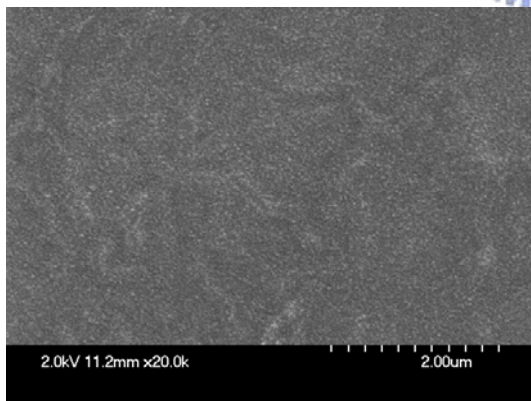
(b)



(c)



(d)



(e)

Fig. 2-15 SEM micrographs showing surface morphology of Si substrate after removal of silicide layer from the 750°C-annealed samples of (a) P2, (b) P2F2, (c) P2F4, (d) P2F5, and (e) P1F5.